Charge Transport through a Novel Zeolite Y Membrane by a Self-Exchange Process

Hyunjung Lee and Prabir K. Dutta*

Department of Chemistry, The Ohio State University, Columbus, Ohio 43210

The preparation of thin ($\sim 1\mu$m), mechanically stable, and relatively pinhole-free zeolitic membranes is described. Nanocrystalline zeolite Y (100−200 nm) is used as the starting material and coated onto a porous alumina substrate. Pinholes within the membrane are filled with a positive photoresist. Upon illumination of the photoresist, only the light-exposed parts are solubilized, whereas the photoresist within the cracks is not affected, thereby sealing them. The leak properties of such membranes were tested using Rhodamine 123 dye, and levels of about 0.5% leaking as compared to the non-photoresist-coated membranes were found. Accessibility of the intrazeolitic volume was examined by ion exchange and for optimally illuminated membranes was comparable to uncoated membranes. Charge transport through the membrane by electron hopping by a self-exchange process involving bipyridinium ions was demonstrated. The electron transfer was initiated using a photochemical $Ru(bpy)_3^{2+}$−EDTA system.

Introduction

Membranes can keep apart two chemical systems that interfere with each other, yet, allowing for transport of specific species through the membrane. Probably, the most celebrated example of membranes is in biological systems, as in a living cell, where the membrane makes it possible for the cell to survive by allowing proper nutrients to pass through the membrane. Membranes also find extensive use in technological applications via selective passage of certain molecules, while excluding others.[1] Our interests have been in the development of artificial photosynthetic systems, where light-activated charge separation can lead to interesting chemistry, including possibly the splitting of water into hydrogen and oxygen.[2] It is well recognized that in order to do so, the photogenerated hole and electron need to be spatially separated, and we are examining zeolite membranes toward this end.[3]

Zeolitic membranes are an active area of research because of their molecular sieving ability.[4] Several methods exist for the preparation of zeolitic membranes, including the direct formation on a substrate using hydrothermal synthesis[5,6] and secondary growth of preformed crystals.[7,8] The potential industrial applications of zeolitic membranes include separations, catalytic reactions, zeolite electrodes, sensors, and ion exchange processes.[9] In cases where different compositions are to be maintained on two sides of a membrane, pinholes that produce pathways for molecules to traverse the membrane need to be eliminated. It is a challenging task to make thin, mechanically stable, and defect-free membranes with access to the pores of the zeolite. Secondary growth,[10] use of binders,[8,11] polymer blending,[12] chemical vapor deposition (CVD),[13] and a post-synthetic coking method[14] are reported to block pinholes as well as improve mechanical stability. Methods such as polymer blending and using a binder to eliminate pinholes introduce the drawback of blocking the zeolite surface and pores.[15]

Most previous studies of zeolite membranes have focused on separations of gases.[4,9] Our interest is to keep species separated in an aqueous medium with ultrathin ($<1\mu$m)

membranes. In this paper, we report the preparation of membranes using nanocrystalline zeolite Y. A photoresist treatment that reduces pinholes, but still allows access to the intrazeolitic volume is described. The mechanical stability is improved upon photoresist coating. Leaks through the membrane and its ion exchange properties have provided information on the nature of defects and the accessibility to zeolite pores after photoresist coating. Demonstration of charge propagation by electron hopping through the membrane is demonstrated using the well-studied photochemical $Ru(bpy)_3^{2+}$−bipyridinium ion system.[2]

Experimental Section

A. Synthesis of Nanocrystalline Zeolite Y. Nanocrystalline zeolite Y was synthesized from clear solutions of tetramethyl-ammonium (TMA)-aluminate according to the patent literature.[16] The TMA-aluminate solution was prepared by dissolving 13.33 g of $Al_2(SO_4)_3 \cdot 18H_2O$ in 70 mL of distilled water, followed by the addition of 25 wt % NH_3 solution to precipitate $Al(OH)_3$. The gel was centrifuged and washed to remove sulfate ions. An amount of 36.46 g of 25 wt % TMAOH solution and distilled water was added to the $Al(OH)_3$ cake to obtain a clear solution. To this solution, 0.0799 g of NaOH in 10 mL of water was added with mixing, followed by the addition of 14.17 g of tetraethylorthosilicate (TEOS). A synthesis solution has the following molar composition: $SiO_2:Al_2O_3 = 3.4$, $Na_2O:Al_2O_3 = 0.05$, $(TMA)_2O:Al_2O_3 = 2.5$, $H_2O:Al_2O_3 = 370$. The synthesis mixture was placed in a Teflon bottle and heated at 100 °C in an oven until white crystals were observed.

B. Zeolitic Film Casting. An amount of 33 mg of calcined, Na^+ ion-exchanged zeolite crystals was dispersed in 10 mL of distilled water. The zeolite suspension was sonicated in a chilled water bath for three hours. A 21 mm diameter aluminum oxide filter membrane (Anodisc, Whatman) was used as a substrate. Zeolite membrane was formed on the surface of an alumina support by dropping 0.125 mL of nanocrystalline zeolite suspension and air-drying it in a covered petri dish. A spin coating procedure (1500 rpm, 10 s) using the same zeolite
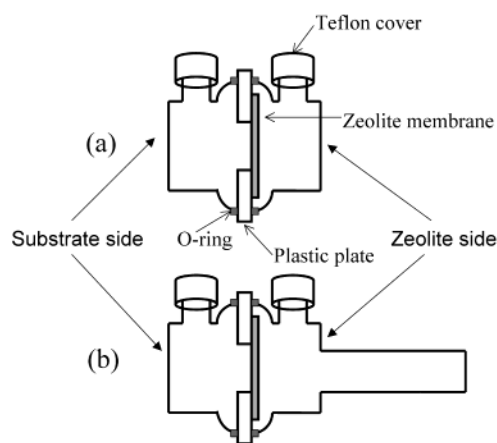
Charge Transport through a Zeolite Y Membrane

J. Phys. Chem. B, Vol. 106, No. 46, 2002 **11899**

Figure 1. (a) Schematic of a two-compartment cell. (b) Modified cell for spectroscopic study. One side has a 1 cm cuvet for absorption measurement.

suspension also worked well. Bipyridinium−zeolite membranes were prepared by starting with bipyridinium ion-exchanged zeolite Y nanocrystals.

C. Photoresist-Coating of the Membrane. A positive photoresist (AZ 7920, Clariant) was coated on the zeolite film by a spin coating method (2000 rpm, 30 s). After solvent evaporation at room temperature, the sample was baked at 80 °C for 10 min and then exposed to ultraviolet light (Mercury I-line lamp, 335 nm) either from the photoresist side or substrate side. The developed portion of the photoresist was removed by treatment with the developing solution (AZ 300 MIF developer, Clariant). The time of exposure to the development solution was done in 20 s increments, followed by water rinsing. Completion of the development process was indicated when the color of the rinsed solution was no longer red. The hard baking procedure involved heat treatment of the membrane at 110 °C for 10 min after the development process.

D. Characterization. X-ray powder diffraction (XRD) patterns were recorded with a Rigaku Geigerflex diffractometer using Ni-filtered Cu Kα radiation (40 kV and 25 mA). Particle and film morphology were obtained using a JEOL 820 scanning electron microscope.

E. Leak Test of the Photoresist-Coated Membrane. The borosilicate glass cell used for these experiments consisted of two halves that were separated by a plastic plate. The zeolitic membrane was attached to the plastic plate by epoxy resin (Super Glue, Pacer Technology), and the plate and the cell parts were secured by two O-rings and a metal clamp. Figure 1a shows a schematic of the cell. The leaking property of the photoresist-coated membranes was tested using a 6.25×10^{-6} M aqueous solution of Rhodamine 123 (Molecular Probe). To measure the leak through the membrane, dye solution was placed on the zeolite side, while the substrate side was filled with distilled water. The solution in the substrate side was sampled every 30 minutes by removing aliquots, and emission spectra were measured using a Spex Fluorolog fluorometer at an excitation wavelength of 480 nm. Samples were returned to the cell after the fluorescence measurement.

F. Ion-Exchange Capacity of the Photoresist-Coated Membrane. Methylviologen (1,1′-dimethyl-4,4′-bipyridinium, MV^{2+})-exchanged zeolitic film was inserted in the cell and 0.05 M NaCl solution was placed in the substrate or zeolite side of the cell to ion exchange the intrazeolitic MV^{2+}. The NaCl solution was sampled every 10 or 20 minutes by UV−visible spectroscopy, and returned to the cell after the measurement.

G. Chemicals. N,N'-Tetramethyl-2,2′-bipyridinium dibromide (DQ^{2+}) was prepared as described by Homer and Tomilson.[17] Propyl viologen sulfonate (PVS) was also prepared following literature procedures.[18] (2,2'-Bipyridyl) ruthenium(II) chloride hexahydrate ($Ru(bpy)_3^{2+}$, Strem Chemicals), Na_2EDTA (GFS Chemicals), and methyl viologen dichloride hydrate (MV^{2+}, Aldrich) were purchased with the highest purity available and used as received.

H. Photolysis. The light source was a xenon arc lamp equipped with a water filter, a 420 nm cutoff filter, and a reflecting mirror (420−650 nm). The power of the radiation incident on the substrate side of the cell was measured by a Coherent 210 power meter to be 250 mW/cm². The cell in Figure 1a was modified to that of Figure 1b. One part now had a built-in (1 cm internal length) cuvet for an in-situ absorption spectroscopic study. This was necessary because of the extreme oxygen sensitivity of bipyridinium radicals and any transfer to an external cell would have led to radical oxidation. A $DQ^{2+}-Y$ membrane was inserted in the cell. An amount of 17 mL of 0.025 M PVS solution was placed in the zeolite side and bubbled with argon. Small amounts of $Ru(bpy)_3^{2+}$ and TEA were added, and the solution was irradiated for 5 minutes to remove trace oxygen. The concentration of $Ru(bpy)_3^{2+}$ and TEA was 8×10^{-6} M and 10^{-3} M, respectively. A small amount of PVS radical was generated and reacted with oxygen in the cell, which was monitored by in-situ UV−visible absorption spectroscopy. After 30 minutes, 10 mL of deoxygenated $Ru(bpy)_3^{2+}$, Na_2-EDTA, and DQ^{2+} solution was added to the substrate side and the solution was irradiated for 80 minutes, during which time the solution on the zeolite side was monitored for PVS radical by UV−visible spectroscopy. The concentration of $Ru(bpy)_3^{2+}$, Na_2EDTA, and DQ^{2+} in the substrate side was 5×10^{-4} M, 0.04 M, and 0.025 M, respectively.

Results

The results are separated into two sections, the first focusing on membrane formation and properties, followed by charge transport studies through the membrane.

A. Zeolite Membrane Formation and Properties. *Membrane Fabrication.* Colloidal crystals of zeolite Y synthesized from clear tetramethylammonium aluminosilicate solutions were used as the starting material.[16] The powder diffraction pattern of the synthesized zeolite matched well with that of zeolite Y. The scanning electron micrograph of the zeolite showed that the particle size was between 100 and 200 nm.

Sixty-micrometer-thick porous alumina with a honeycomb pore structure of 0.2 μm (determined by SEM) was used as substrates. Zeolitic films on these substrates were prepared by either spin coating or solvent evaporation. Typically, a 0.125 mL portion of a suspension of 33 mg of zeolite particles in 10 mL of distilled water formed a 1 μm thick zeolite layer. The thickness of the zeolite layer could be controlled by the number of coatings or by the concentration of zeolite suspension.

Positive-type photoresist liquid was dropped on the zeolite film, followed by exposure to ultraviolet radiation. The composition of the photoresist liquid is proprietary, but it is known from the patent literature that it contains an organic resin, sensitizer, solvents, and additives.[19] Illuminated photoresist dissolves upon treatment with the development solution. Figure 2 is an SEM image of the top view and the cross-section of a photoresist-coated zeolite Y membrane. The membrane is composed of 7−8 layers of nanometer-sized zeolite crystals on top of the substrate, with a thickness of about 1 μm. The side
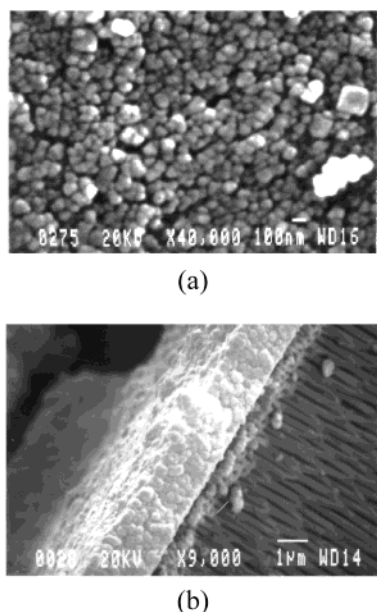
Figure 2. SEM micrograph of photoresist-coated zeolite membrane: (a) top view, (b) side view.

view shows the pores of the substrate. The top view does not show a photoresist layer, since the photoresist penetrates into the membrane.

Leak Properties of the Photoresist-Coated Membrane. Rhodamine 123 was selected for the leak test since it has a larger kinetic diameter (>10Å) than the 12-membered rings (7.4Å) of the zeolite and can only cross the membrane through pinholes. Figure 3a compares the emission from the dye that has traversed across a non-coated zeolitic membrane and photoresist-coated (20 s irradiated) membrane. Photoresist-coated membrane has less than 0.5% of leaking as compared to that of the non-coated film, which indicates that the photoresist is effectively blocking the pinholes.

In order to optimize the leak properties of the membrane, a series of membranes with different irradiation times were prepared and their leak properties tested. Figure 3b compares the change in leaking of Rhodamine 123 as the irradiation time was increased. Films irradiated for 20 s showed leaks comparable to those of the non-irradiated film, whereas films irradiated for 40 or 60 s showed considerable more leaking (a factor of four after 3 h). By virtue of the nature of positive photoresist, longer irradiation times result in solubilization of more photoresist, leading to a decrease in the amount of photoresist in the pinholes, and more leaking. Therefore, the optimum duration of illumination appears to be 20 s. Heating the developed membrane to 110 °C (hard baking) did not improve the leaking property.

Ion-Exchange Properties of the Photoresist-Coated Membrane. Ion-exchanging experiments were carried out to test if the interior of the zeolite was accessible after photoresist coating and development process. First, the ion-exchange capacity of the blank alumina substrate coated with photoresist was examined. The probe for monitoring accessibility was the methylviologen ion (MV^{2+}) which has an absorption band at 290 nm and can be readily quantitated. The photoresist and alumina substrate does not have a measurable ion-exchange capacity.

For the membranes, the zeolite crystals were ion exchanged with MV^{2+} prior to casting. If zeolitic pores were inaccessible, then MV^{2+} would not be ion exchanged out of the zeolite by Na^+ in the solution. Figure 4a shows the amount of MV^{2+}
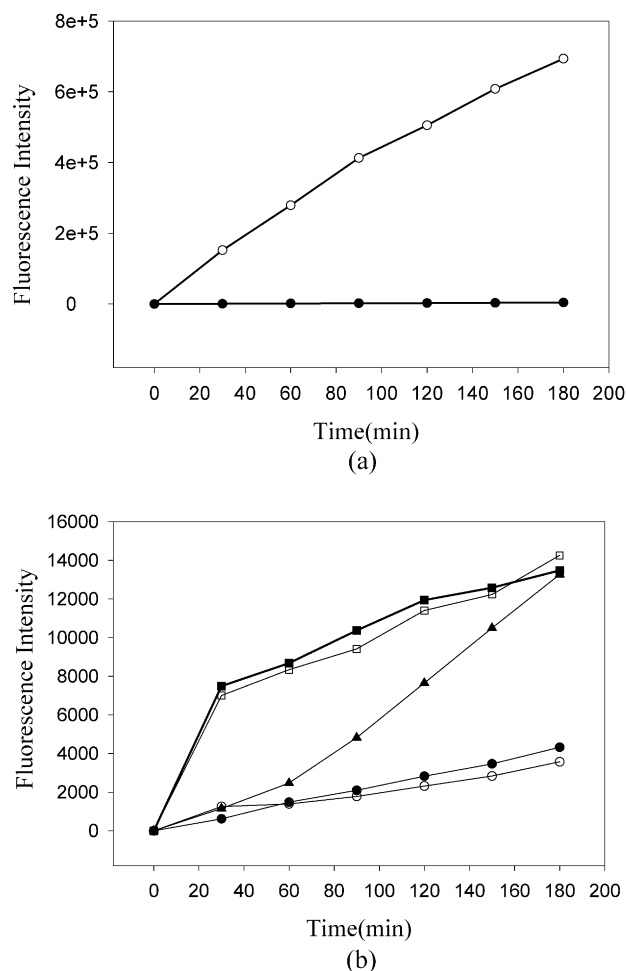

Figure 3. Fluorescence spectra of rhodamine dye leaking through membranes (a) ○: zeolite membrane without photoresist coating, ●: leaking through photoresist-coated zeolite membrane; (b) photoresist-coated zeolite membrane with various irradiation time, ○: no irradiation, ●: irradiation for 20 s, ▲: irradiation for 20 s followed by hard baking, ■: irradiation for 40 s, □: irradiation for 60 s.

ion-exchanged into the NaCl solution in contact with the zeolitic membrane as a function of time. The kinetics of ion exchange followed a biphasic behavior with rapid exchange over a 20−30 minute period followed by a slower exchange process over an hour before steady state was reached. A membrane without any irradiation or irradiated for 20 s shows the maximum amount of recovered MV^{2+}, and as the irradiation time increased, the recovery decreased. This observation appears contrary to expectation since longer irradiation should remove more photoresist and produce a more accessible membrane. We propose that the lower recovery arises because of less MV^{2+} in the membrane. The development solution contains tetramethylammonium hydroxide (TMAOH), and for samples with longer irradiation times, longer exposure to TMAOH was required to remove the soluble photoresist. During the development process, TMA^+ cations can ion exchange into the zeolite, replacing MV^{2+}; the longer the membrane was in TMAOH, the more MV^{2+} will be removed from the zeolite. This was confirmed by re-ion exchanging a 40 s-irradiated membrane with MV^{2+}, and recovering the MV^{2+} from the membrane by treatment with NaCl. It was found that the amount of recovered MV^{2+} reached the same level as a non-irradiated or 20 s-irradiated membrane (data not shown). Figure 4a also shows that membranes with no irradiation or 20 s of irradiation had similar absolute recovery of MV^{2+}, although the dynamics
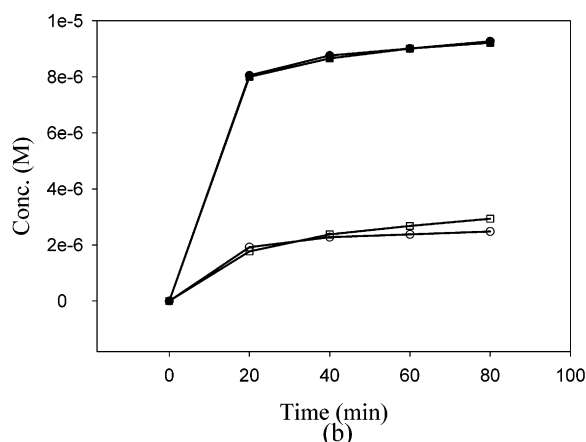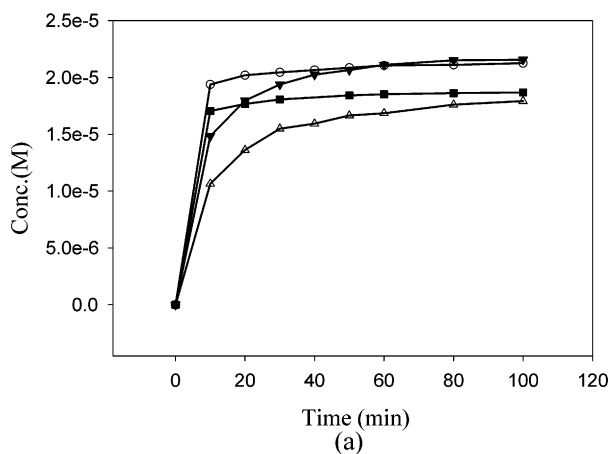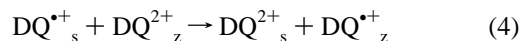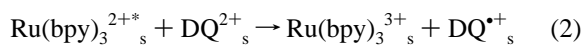
Charge Transport through a Zeolite Y Membrane
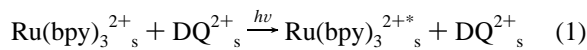
J. Phys. Chem. B, Vol. 106, No. 46, 2002 **11901**

Figure 4. MV^{2+} ion exchange experiment with photoresist-coated zeolite membrane (a) from zeolite side, ▼: no irradiation, ○: irradiation for 20 s, ■: irradiation for 40 s, △: irradiation for 60 s; (b) from substrate side, ●: zeolite membrane without photoresist coating, ○: photoresist-coated zeolite membrane without substrate side irradiation, □: substrate side irradiation for 10 s , ■: substrate side irradiation for 40 s.

was slower in the non-irradiated case. This indicates that in the as-prepared samples, photoresist is partially blocking zeolite access.
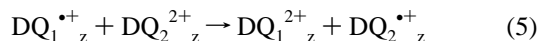
The accessibility of molecules within the zeolite from the alumina substrate side of the membrane is shown in Figure 4b. The recovery is low if there is no irradiation. Upon irradiation for 40 s, the membrane was as accessible as one without photoresist coating. Thus, it appears that 20 s of irradiation from the zeolite side and 40 s of irradiation from the substrate side resulted in optimum zeolitic membranes. Such a membrane showed leaking (0.5%) similar to that of the 20-s zeolite-side irradiated membrane. Therefore, irradiation from the alumina side removes excess photoresist that has penetrated through the zeolite pinholes into the substrate.

B. Charge Transport Studies with the Photoresist-Coated Membrane. The possibility of charge transport through the zeolitic membranes was investigated by using a reaction that involves electron transfer by a self-exchange mechanism and initiated by a photochemical process. The photochemical system included a zeolite membrane that was ion-exchanged with the bipyridinium ion (DQ^{2+}). On the substrate side of the membrane, $Ru(bpy)_3^{2+}$ (5×10^{-4} M) , DQ^{2+} (0.025 M), and Na_2EDTA (0.04 M) were introduced. On the zeolite side, another bipyridinium ion, neutral propyl viologen sulfonate (PVS) solution (0.025 M) was introduced. The basic reactions involved in the process are as follows:
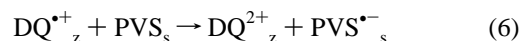
Substrate side:

$$Ru(bpy)_3{}^{2+}{}_s + DQ^{2+}{}_s \xrightarrow{hv} Ru(bpy)_3{}^{2+*}{}_s + DQ^{2+}{}_s \quad (1)$$

$$Ru(bpy)_3{}^{2+*}{}_s + DQ^{2+}{}_s \rightarrow Ru(bpy)_3{}^{3+}{}_s + DQ^{\bullet+}{}_s \quad (2)$$

$$Ru(bpy)_3{}^{3+}{}_s + EDTA \rightarrow Ru(bpy)_3{}^{2+}{}_s + EDTA_{ox}{}^+ \quad (3)$$

$$DQ^{\bullet+}{}_s + DQ^{2+}{}_z \rightarrow DQ^{2+}{}_s + DQ^{\bullet+}{}_z \quad (4)$$

Intrazeolitic membrane:

$$DQ_1{}^{\bullet+}{}_z + DQ_2{}^{2+}{}_z \rightarrow DQ_1{}^{2+}{}_z + DQ_2{}^{\bullet+}{}_z \quad (5)$$

Zeolite side:

$$DQ^{\bullet+}{}_z + PVS_s \rightarrow DQ^{2+}{}_z + PVS^{\bullet-}{}_s \quad (6)$$

where the subscripts "s" and "z" represent solution and zeolite, respectively.

If charge transport through the zeolite membrane can occur by electron hopping via the self-exchange of ion-exchanged DQ^{2+}, as shown in eq 5, then illumination of the substrate side of the membrane should lead to creation of a PVS radical on the zeolite side of the membrane and measure of this radical was the focus of these experiments. The process is schematically represented in Figure 5.

However, there were several problems that needed to be addressed. First, as shown in Figure 3, though application of the photoresist decreased the level of leaking through the membrane, it did not completely seal it. Second, no matter how tight the seals were of the cell (Figure 1b), it was impossible to keep O_2 from leaking into the cell and reacting with the bipyridinium radical. Thus, we needed to come up with an appropriate blank system to demonstrate the influence of leaking and control the effect of oxygen. In order to accomplish that, the blank (or control) membrane we designed was an alumina substrate coated with photoresist alone and cured as described before. For ensuring that the effect of O_2 leaking into the zeolite side was controlled, a small amount of $Ru(bpy)_3^{2+}$ (8×10^{-6} M) and triethanolamine (TEA, 10^{-3} M) was introduced into the deaerated PVS solution on the zeolite side and photolyzed for 5 min. A PVS radical was generated and reacted with oxygen in the system, which was monitored by UV−visible absorption spectroscopy for 30 minutes. This data, shown in Figure 6a, demonstrated that the bipyridinium radical that is produced decays with time, as O_2 leaks into the cell. However, the constant presence of radical indicates that O_2 is being contained. Figure 6a also shows that the concentration of $Ru(bpy)_3^{2+}$ during this time remains constant. After 30 minutes, $Ru(bpy)_3^{2+}-DQ^{2+}-Na_2EDTA$ was added to the substrate side (time indicated by arrow in Figure 6) and photolyzed with visible light while the absorption spectrum of the solution on the zeolite side was monitored for the next 80 minutes. There is a slight increase in the $Ru(bpy)_3^{2+}$ on the zeolite side as a result of leaking. The viologen radical, however, continues to decrease though there is leak of $DQ^{\bullet+}$ through the membrane and formation of $PVS^{\bullet-}$ on the zeolite side, indicating a continuous oxygen leak into the cell. After 30 minutes, the decrease of the amount of slowed, because of the $DQ^{\bullet+}$ leak.

The same experiment was repeated with the photoresist-coated DQ^{2+}-exchanged zeolite membrane, and the data is shown in Figure 6b. Before the addition of the $Ru(bpy)_3^{2+}-DQ^{2+}$ solution on the substrate side (first 30 minutes), the behavior was very
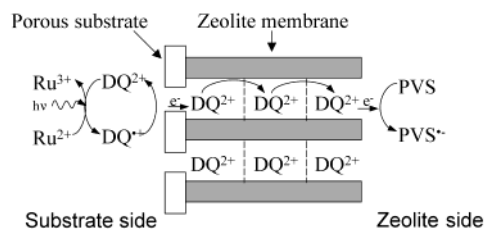
Figure 5. Charge transport through a zeolite Y membrane.

similar to that of the blank membrane, as far as the leak of O_2 into the cell. However, after the Ru(bpy)$_3{}^{2+}-$ DQ$^{2+}-$ Na$_2$EDTA addition and initiation of photolysis, there was a linear growth of PVS$^{\bullet-}$ radical on the zeolite side beginning at about 45 minutes. Because the blank sample with similar leak properties does not show the increase of PVS$^{\bullet-}$ radical, this radical must be forming due to charge transport across the zeolite membrane.

A similar experiment was repeated with a photoresist-coated MV^{2+}-exchanged zeolite membrane with Ru(bpy)$_3{}^{2+}-$MV$^{2+}-$Na$_2$EDTA on the substrate side, and the data are shown in Figure 6c. The O_2 leak prior to addition of Ru(bpy)$_3{}^{2+}-$MV$^{2+}-$Na$_2$EDTA (first 30 minutes) was somewhat more than the previous two membranes and reflects the variability in controlling the O_2 leak. The leak of Ru(bpy)$_3{}^{2+}$ through the membrane was comparable. However, similar observations were made in that the PVS$^{\bullet-}$ radical increased dramatically after creation of MV$^{\bullet+}$ radical on the substrate side.

Discussion

Membrane Preparation: Photoresist Strategy. The strategy that we have taken to make defect-free zeolitic membranes is assembly of crystals on a substrate and sealing the gaps between crystals with a filler. Limitations of such methods in the past have been the potential clogging of zeolite pores and covering of the zeolite surfaces by the additive.[15] We have circumvented this problem by using photoresist to fill the inter crystal spaces. Photoresist is frequently used for lithography or micro patterning.[19] Positive photoresists are made up of sensitizers, resins, solvents, and additives. The sensitizers are typically diazonaphthoquinones (DNQ) dispersed in a low molecular weight phenolic matrix resin (Novolak). Because of the hydrophobic nature of DNQ, it acts as a dissolution inhibitor of the resin. Upon irradiation, the DNQ is converted to the hydrophilic indenecarboxylic acid which renders the exposed film (sensitizer + resin) soluble in the developer (0.2−0.3 M TMAOH).[20]

Since the photoresist is liquid before the heat treatment, it can flow into pinholes between crystals. The typical photoresist coating process involves coating−soft baking−irradiation−development−hard baking. Upon soft baking the photoresist-coated zeolitic membrane at 80 °C, the organic resin solidifies and becomes insoluble. Upon irradiation, the exposed photoresist becomes soluble and the development process removes the reacted photoresist, as schematically depicted in Figure 7. The mechanical stability of the membrane is improved upon coating. The only other example of using a photoresist to fill grain boundaries has been between diamond crystals to achieve a high-performance film for an electric device.[21]

On the basis of the amount of zeolite that was used to make the membrane, and assuming a maximum loading of 1.5 molecules of methyl viologen per supercage, we estimate from Figure 4 that about 83% of the MV^{2+} is ion-exchanged from the membrane. The recovery of the ion exchange from the uncoated and photoresist-coated zeolitic membranes were comparable, indicating that the coating was not blocking zeolite access.
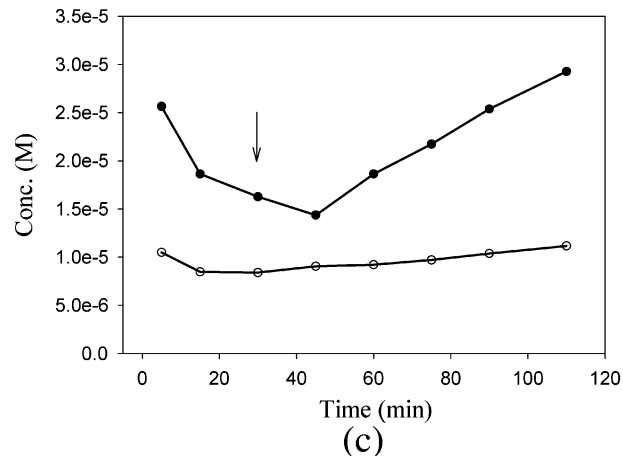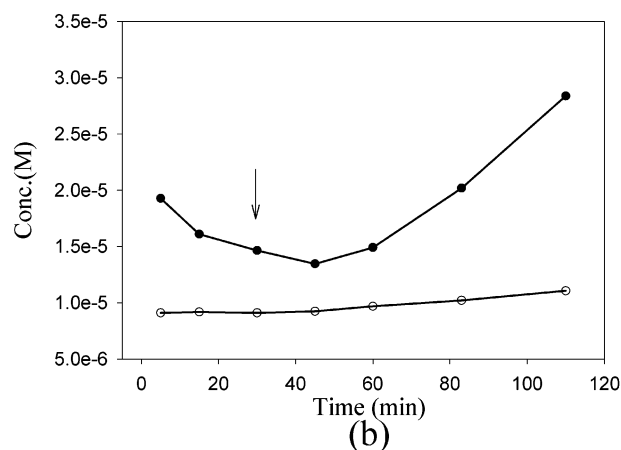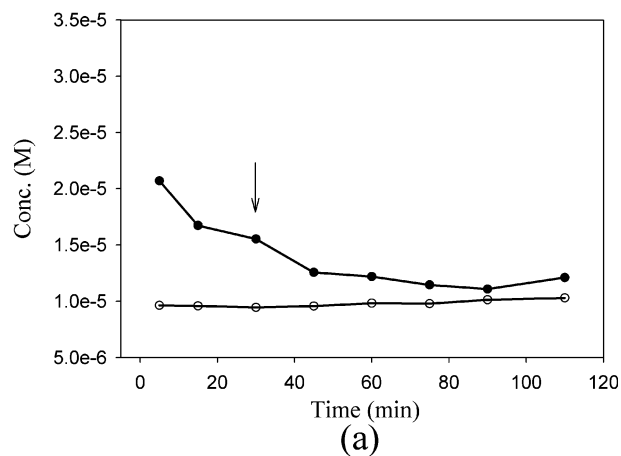

(a)

(b)

(c)

Figure 6. Measure of PVS$^{\bullet-}$ generation at the zeolite side. Arrow indicates the point where Ru(bpy)$_3{}^{2+}-$MV^{2+} or DQ$^{2+}-$EDTA solution is added in the substrate side (a) blank experiment with photoresist-coated alumina substrate (b) with photoresist-coated zeolite membrane, DQ^{2+} was used for electron relay (c) with photoresist-coated zeolite membrane, MV^{2+} was used for electron relay.

Complete exchange of the MV^{2+} from the membrane by 0.1 M NaCl took about 60 minutes before steady state was reached. For the same amount of zeolite in powder form, the process is instantaneous. This is indicative of the fact that ion-exchange from the membrane proceeds from the surface layer of zeolite, since the access of NaCl is limited only to this layer. In the particular membranes that we have studied, there are about seven layers of zeolite crystallites, so interparticle ion exchange needs to occur.

Interparticle ion exchange has been noted between mixtures of Li$^+$- and Na$^+$-zeolite A, and the rate was controlled by zeolite
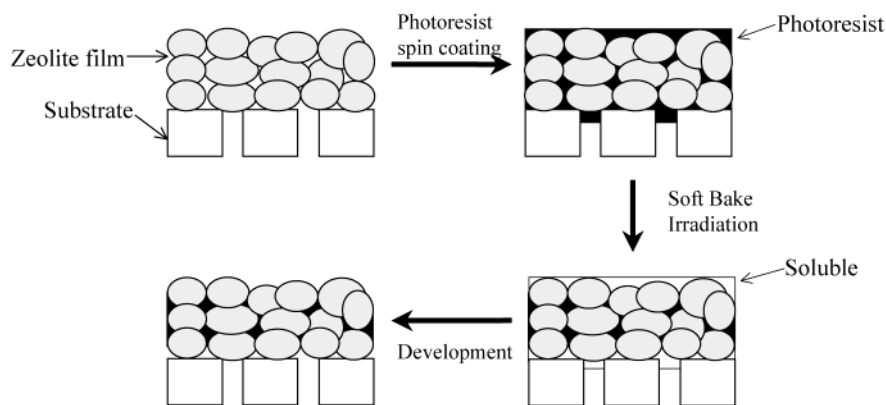
Charge Transport through a Zeolite Y Membrane

J. Phys. Chem. B, Vol. 106, No. 46, 2002 **11903**

Figure 7. Photoresist coating process.

crystallite size and degree of hydration.[22] Small crystals (1−2 μm) were found to reach equilibrium almost instantaneously upon mixing, whereas larger crystals (20−25 μm) took 24 hours. In comparison to these studies done with vigorous mixing of powders, if the crystals (1−2 μm) are simply gently brought together, then the process can take up to 24 hours to come to equilibrium. With the present nanocrystalline zeolite Y membranes, 60 minutes is required to reach equilibrium. This is consistent both from the smaller size of crystallites ($\sim$100 nm) as well as the static conditions under which the experiment is done. Thus, the ion-exchange process can be viewed as the first layer of crystallites rapidly exchanging their MV^{2+} with Na^+ in solution, followed by a slower process of interparticle ion exchange.

Charge Transport through Zeolitic Membrane. Our objective was to examine if charge transport is possible through zeolitic membranes via electron self-exchange of bipyridinium ions. There is enough evidence both in the polymer-based electrochemical and zeolite literature that charge hopping between bipyridinium ions can be efficient. The ability to transport charge by self-exchange at rates significantly higher than physical diffusion has been noted on polymer electrodes.[23] Voltammetric studies have provided estimates of electron self-exchange rates of bipyridinium ions in poly(ethylene glycol) films.[24] For MV^{2+}, the self-exchange rate constant for MV^{2+}/$MV^{\bullet+}$ exchange depended on the ionic strength of the medium, but varied from 8.6×10^4 to 1.6×10^5 M^{-1} s^{-1}.[24]

Yoon et al. noted that carbonylmanganate ions (Mn-$(CO)_4P(OPh_3)^-$) too large to enter the zeolite can effectively reduce all of the intrazeolitic MV^{2+}. The proposed mechanism involved reduction of MV^{2+} only at the zeolite periphery (about 1% of MV^{2+}) followed by self-exchange that moved the reduced charge to the interior of the zeolite.[25] The complete reduction of all the intrazeolitic viologen in a zeolite crystallite occurred very fast.

Several studies have reported that reduced bipyridinium ions within individual zeolite particles can transport charge via self-exchange and can exchange charge with bipyridinium ions external to the zeolite in solution.[26,27] These studies were the basis for the use of photoresist-coated DQ^{2+}−Y membrane for electron transport. Comparison of the blank experiments with the bipyridinium-exchanged zeolites clearly establishes that trans membrane charge transfer is occurring. As an electron moves from one side of the membrane to the other side, cation transport needs to occur to maintain charge neutrality. We propose that the Na^+ cation from the sacrificial electron donor (Na_2EDTA) accompanies the electron, keeping the charge balance. When TEA (triethanolamine) was used for a sacrificial electron donor

on the substrate side, no "net" PVS radical was observed, because of the absence of Na^+ that can accompany the electron transfer.

Ion exchange of intrazeolitic DQ^{2+} by sodium cation in solution can take place, which will remove acceptors from the zeolite. Indeed, we found that even though the experiment was started with a loading of 1 DQ^{2+} per supercage, at the end of the experiment, only about 0.7 molecules of DQ^{2+} per supercage were left. Though it might appear that at least one viologen molecule per supercage is required for charge hopping to proceed, if charge hopping occurs by a percolation route, then loading levels can be considerably lower. Because of the high loading of the intrazeolitic bipyridinium ions, physical diffusion of the radical across a zeolite particle is expected to be quite small (with diffusion coefficients of 10^{-8} cm^2/s, or even smaller).[28] Thus, we can view the process as electron hopping between immobile bipyridinium ions. The diffusion coefficient for such a process is similar to that for polymeric electrodes and is given by

$$D_{app} = \frac{k_{ex}\delta^2 c}{6}$$

where k_{ex} is the second-order self-exchange constant, δ is the distance between the centers of the bipyridinium ions, and c is the concentration of the redox species. Hui and Baker have used this model for electron transport through MV^{2+}−zeolite Y electrodes.[29] Such a model of charge transport can be viewed as a percolation problem. The supercage arrangement in a zeolite Y crystal is the same as the diamond lattice. The percolation threshold of diamond lattice is 0.428, indicating that when occupancy of sites exceeds this number, there is a cluster extending throughout the crystallite.[30] So, at a loading level of 0.7 DQ^{2+} per supercage, percolative pathways that can promote charge transport via self-exchange will exist. This is also an advantage with a multidimensional zeolite, where three-dimensional connections can provide many trans-membrane pathways, as compared to a one-dimensional zeolite such as zeolite L.

The rates of $PVS^{\bullet-}$ generation between the DQ^{2+} and MV^{2+} membranes are comparable. This is puzzling, considering that there is a stronger driving force for electron transfer between $DQ^{\bullet+}$ and PVS as compared to $MV^{\bullet+}$ and PVS. These results indicate that the limiting step in the charge transport process is inter-zeolitic self-exchange, since it is known that charge transport within the zeolite for the bipyridinium ions is fast.[25] There are about 7 layers of crystallites that the charge has to propagate through to cross the membrane. At the interface between two crystallites, the charge has to hop between the

Lee and Dutta

bipyridinium ions on the two crystallites and, unlike the zeolite interior, where the packing of the ions is dense, there are fewer ions on the crystallite surface. This will slow down the process of charge transport and is the rate-limiting step in the process.

Another possibility for formation of PVS$^{\bullet-}$ is that the DQ$^{\bullet+}$ or MV$^{\bullet+}$ on the zeolite side ion-exchange into the zeolite membrane, replacing the DQ^{2+} or MV^{2+}, and eventually these ion-exchanged species penetrate through the membrane and show up on the substrate side and transfer an electron to PVS. However, this is unlikely, because we have determined that in the MV^{2+} system, the concentration of MV$^{\bullet+}$ to MV^{2+} on the substrate side is about 0.005, indicating that there is considerably more MV^{2+} and Na$^+$ in the system than there is MV$^{\bullet+}$ and therefore the possibility of replacement of MV^{2+} in the zeolite by MV$^{\bullet+}$ by ion exchange is unlikely. Though we have not calculated the amounts of DQ$^{\bullet+}$, we expect the scenario to be similar to that of the MV^{2+} system.

There are other examples of electron transfer across membranes. Lawson et al. utilized a doped polypyrrole film to separate a solution of electron donor from a solution of an electron acceptor.[31] Because the conductive polymer is both electronically and anionically conductive, the membranes could transport electrons from the donor solution to the acceptor solution, and anions in the opposite direction. Matsumara et al. used conducting polymer films loaded with titanium dioxide or cadmium sulfide particles for photocatalytic electron and proton pumping across the membrane.[32] The electron transfer occurred by the electron flow in these cases, not electron hopping through acceptors. Thus, the data presented in this paper is the first report of electron transfer through a membrane via a charge hopping process.

Conclusions

We have shown that the pinhole defects in a zeolite membrane can be reduced effectively with a positive photoresist coating and development process, and leaves the surface and zeolitic pores accessible, as evidenced from ion-exchange studies. The photoresist coating also improves the mechanical stability of the membrane. The illumination period and development conditions are important factors that need to be optimized to get effective pinhole blocking. These membranes were used to demonstrate charge transport across the membrane by electron self-exchange of bipyridinium ions within the zeolite. A photochemical Ru(bpy)$_3$$^{2+}$−EDTA system was used to initiate the charge transport process.

References and Notes

(1) Mulder, M. *Basic Principles of Membrane Technology*; Kluwer Academic Publishers: Dordrecht, 1991.

(2) Vaidyalingam, A. S.; Coutant, M. A.; Dutta, P. K. *Electron-transfer processes in zeolites and related microheterogeneous media*; Balzani, V., Ed.; Wiley-VCH: New York, 2001; Vol. 4, pp 412−487.

(3) Castagnola, N. B.; Dutta, P. K. *J. Photosci.* **1999**, *6*, 91.

(4) Caro, J.; Noack, M.; Kolsch, P.; Schafer, R. *Microporous Mesoporous Mater.* **2000**, *38*, 3.

(5) Lee, H.; Dutta, P. K. *Microporous Mesoporous Materials* **2000**, *38*, 151.

(6) Jia, M. D.; Chen, B.; Noble, R. D.; Falconer, J. L. *J. Membr. Sci.* **1994**, *90*, 1.

(7) Gouzinis, A.; Tsapatsis, M. *Chem. Mater.* **1998**, *10*, 2497.

(8) Lovallo, M.; Tsapatsis, M. *Chem. Mater.* **1996**, *8*, 1579.

(9) Tavolaro, A.; Drioli, E. *Adv. Mater.* **1999**, *11*, 975.

(10) Nair, S.; Lai, Z. P.; Nikolakis, V.; Xomeritakis, G.; Bonilla, G.; Tsapatasis, M. *Micrporous Mesoporous Mater.* **2001**, *48*, 219.

(11) Le Van Mao, R.; Rutinduka, E.; Detellier, C.; Gougay, P.; Hascoet, V.; Tavakoliyan, S.; Hoa, S. V.; Matsuura, T. M. *J. Mater. Chem.* **1999**, *9*, 783.

(12) Boom, J. P.; Punt, I. G. M.; Zwijnenberg, H.; de Boer, R.; Bargeman, D.; Smolders, C. A.; Strathmann, H. *J. Membr. Sci.* **1998**, *138*, 237.

(13) Nomura, M.; Yamaguchi, T.; Nakao, S.-I. *Ind. Eng. Chem. Res.* **1997**, *36*, 4217.

(14) Yan, Y.; Davis, M. E.; Gavalas, G. R. *J. Membr. Sci.* **1997**, *123*, 95.

(15) Bein, T. *Chem. Mater.* **1996**, *8*, 1636.

(16) Otterstedt, J. E.; Sterte, J.; Schoeman, B. J. International Patent, WO 94/05597, 1994.

(17) Homer, R. F.; Tomilson, T. E. *J. Chem. Soc.* **1960**, 2498.

(18) Willner, I.; Ford, W. E. *J. Heterocyclic Chem.* **1983**, *20*, 1113.

(19) Deforest, W. S. *Photoresist*; McGraw-Hill, Inc.: New York, 1975.

(20) Wallraff, G. M.; Hinsberg, W. D. *Chem. Rev.* **1999**, *99*, 1801.

(21) Yamazaki, S. U.S. Patent 5,036,373, July 1991.

(22) Fyfe, C. A.; Kokotailo, G. T.; Graham, J. D.; Browning, C.; Gobbi, G. C.; Hyland, M.; Kennedy, G. J.; DeSchutter, C. T. *J. Am. Chem. Soc.* **1986**, *108*, 522.

(23) Wooster, T. T.; Watanabe, M.; Murray, M. R. *J. Phys. Chem* **1992**, *96*, 5886.

(24) Gu, N.; Dong, S. *Electrochem. Commun.* **2000**, *2*, 713.

(25) Yoon, K. B.; Park, Y. S.; Kochi, J. K. *J. Am. Chem. Soc.* **1996**, *118*, 12710.

(26) Borja, M.; Dutta, P. K. *Nature* **1993**, *362*, 43.

(27) Sykora, M.; Kincaid, J. R. *Nature* **1997**, *387*, 162.

(28) Walcarius, A.; Lamberts, L.; Derouane, E. G. *Electrochim. Acta* **1993**, *38*, 2276.

(29) Hui, T.; Baker, M. D. *J. Phys. Chem. B* **2002**, *106*, 827.

(30) Stauffer, D. *Introduction to Percolation Theory*; Taylor and Francis: London, 1985.

(31) Lawson, D. R.; Liang, W.; Martin, C. R. *Chem. Mater.* **1993**, *5*, 400.

(32) Matsumra, M.; Ohno, T.; Saito, S.; Ochi, M. *Chem. Mater.* **1996**, *8*, 1370.